

## UVA and UVC modification of photo polymeric surface and application for flexographic deposition of thin coatings

Tamara Tomašegović,<sup>1</sup> Sanja Mahović Poljaček,<sup>1</sup> Mirela Leskovic<sup>2</sup>

<sup>1</sup>Department for Graphic Materials and Printing Plates, University of Zagreb, Faculty of Graphic Arts, Getaldićeva 2, Zagreb, 10000, Croatia

<sup>2</sup>Department of Surface Engineering of Polymer Materials, University of Zagreb, Faculty of Chemical Engineering and Technology, Trg Marka Marulića 19, Zagreb, 10000, Croatia

Correspondence to: T. Tomašegović (E-mail: ttomaseg@grf.hr)

**ABSTRACT:** The object of this research was to perform, characterize, and apply the functional modification of flexographic photo polymeric printing plate surface by UVA and UVC post-treatments. Photo polymeric printing plates have an important application in functional printing, where new printing inks/coatings and substrate formulations are used and the specific qualitative requirements must be met. The limitations of materials and processes often require expensive reformulations of the functional inks to achieve printability. Results of this research showed that the modification of the photo polymeric printing plate surface at the end of its production process can be used to precisely adjust the printing ink transfer to the printing substrate and thus eliminate the need for changing the ink/coating composition. By applying specific UV post-treatment, one can create a flexographic coating deposition system of tailored properties adjustable to variable reproduction systems with high quality requirements. © 2016 Wiley Periodicals, Inc. *J. Appl. Polym. Sci.* **2016**, *133*, 43526.

**KEYWORDS:** crosslinking; photopolymerization; surfaces and interfaces; swelling

Received 5 November 2015; accepted 9 February 2016

DOI: 10.1002/app.43526

### INTRODUCTION

Elastomeric styrene-diene-styrene based photo polymeric materials used in flexography have an irreplaceable role in massive production of thin coatings and prints of high quality used in functional printing (Organic Light Emitting Diodes (OLEDs), biosensors, Radio Frequency Identification (RFID) tags, batteries, solar cell components, and printing for medical applications).<sup>1–4</sup> Named applications require uniformity and specific thickness of printed ink/coating layer to obtain functionality.<sup>5</sup> Due to the limitations of the materials and processes in the production of functional prints, complicated reformulations of the functional ink or specific treatments of the printing substrate often have to be performed.<sup>6,7</sup>

Specifically, when printing conductive components (such as RFID and batteries), the ink/coating thickness must be sufficient to obtain conductivity. The ink/coating thickness depends on the type of the printing ink used, parameters of the printing process, and the roughness and porosity of the printing substrate. The optimal value of the ink/coating thickness can be  $>5 \mu\text{m}$ .<sup>8</sup> However, for OLED printing, ink/coating thickness must be  $<100 \text{ nm}$ .<sup>9</sup> Uniformity of the deposited ink/coating is a cru-

cial feature, as well. Variations of ink/coating thickness can result with detrimental shorts in the deposited coating, and the inconsistently printed continuous fine lines, which lose the conductive properties.<sup>10</sup>

Flexographic printing is highly applicable technique for depositing functional coatings.<sup>11,12</sup> Printing plate for flexographic printing is usually composed of elastomeric, styrene-diene-styrene based photo polymeric sheet on a polyethylene terephthalate (PET) base. It is a carrier of the image transferred to the printing substrate in the reproduction process. Due to the printing plate's elastic deformation during the engagement in the printing process, the contact area between the printing plate and printing substrate ensures the optimal transfer of the printing ink. Flexographic printing plates are extremely durable (run length  $>1,000,000$  prints), can print flat, continuous lines and areas, and their mechanical properties enable printing on a wide range of printing substrates.<sup>13</sup>

In the production of the flexographic printing plate (Figure 1), photo polymeric material is exposed to UVA radiation with wavelength of 365 nm to form the polymerized elements by radical polymerization. These elements will transfer the printing ink to the printing substrate.<sup>13</sup> In the post-treatment [Figure

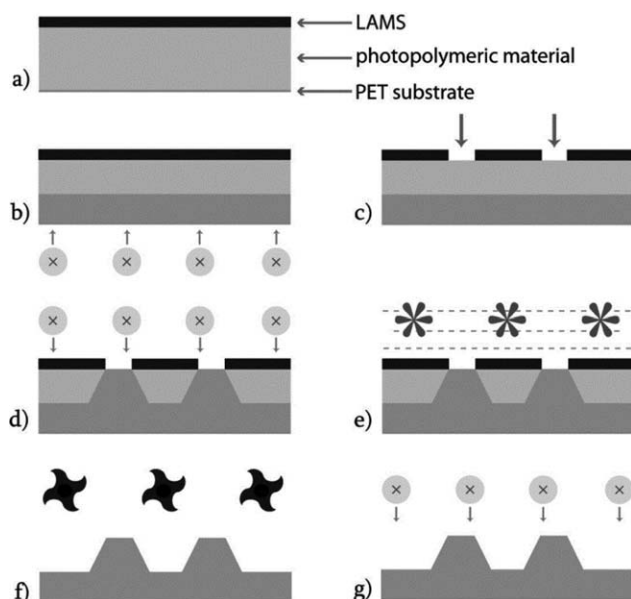


**Figure 1.** Production of photo polymeric flexographic printing plate: (a) photo polymeric sheet prepared for the image transfer, (b) back-exposure (UVA), (c) removing the laser ablation mask layer (LAMS) – image transfer, (d) main exposure (UVA), (e) rinsing, (f) drying, and (g) UVA and UVC post-treatment.

1(g)], polymerized area is exposed to a combination of UVA and UVC wavelengths (365 nm and 254 nm) to terminate the crosslinking process.<sup>13,14</sup> The post-treatment enhances the surface properties of the material, eliminates the stickiness, and defines the surface free energy ( $\gamma$ ) of the printing plate.<sup>14</sup> Recommendations of the printing plate manufacturer are usually followed when adjusting the duration of the UV post-treatments. The surface free energy ( $\gamma$ ) of the flexographic printing plate has to be specifically adjusted to the printing ink and the printing substrate used. In conventional printing (mostly in the packaging production), formulations of inks as well as properties of the printing plate and of the substrate are standard and compatible.<sup>15,16</sup>

However, in functional printing, new types of printing inks/coatings have been introduced.<sup>17,18</sup> Depending on their composition and application, their surface properties can differ a lot from the properties of the conventional flexographic inks, which have the properties adjusted to the photo polymeric printing plates that have relatively low  $\gamma$  (approx.  $30 \text{ m Nm}^{-1}$  –  $40 \text{ m Nm}^{-1}$ ).<sup>19,20</sup> In the dynamic process like printing,  $\gamma$  of both printing plate and printing ink have an important role in obtaining the optimal qualitative properties of the final product. If  $\gamma$  of the printing plate is lower than  $\gamma$  of the printing ink, poor wetting could result with poor quality of the print.<sup>20</sup>

When developing and using functional inks in flexographic printing, their composition is often modified to achieve compatibility with the printing plate in terms of printability.<sup>21</sup> This adjustment can have a negative impact on ink's functional properties and the quality of the final product.

This research proposes and characterizes an alternative, quick, and production workflow-incorporable method for improving

the quality of the coatings printed with functional inks and flexographic inks with higher surface tension than conventional ones. The improvement of the printed ink/coating quality is achieved by functional modification of the flexographic printing plate's surface, performing the additional UV post-treatments (instead of modifying the printing formulation of the printing ink).

The main object of this research was to perform, characterize, and apply the functional modification of flexographic photo polymeric printing plate surface by UVA and UVC post-treatments. The main point was to propose the new method for tailoring the properties of the deposited ink/coating on the print.

In this research, modification of the printing plate's surface was performed in the last step of the printing plate production [Figure 1(g)], where the durations of UVA and UVC post-treatments were varied to influence  $\gamma$  of photo polymeric material, therefore enabling controlled adjustment to the specific quality requirements in the printing process. However, the important aim of this research was to retain the functionality of printing plate after the surface modifications. The properties of the printing plate important in the reproduction process (mechanical stability, non-sticky surface, limited swelling in washing agent, and distribution of dispersive and polar component of  $\gamma$ ) needed to be retained. Due to the potential destructive influence of prolonged UV radiation on the photo polymeric material, the potential start of the degradation process needed to be detected, as well.<sup>22</sup>

Calculations of  $\gamma$  of treated printing plates showed the expected general increase with prolonged UV post-treatment, which affected the ink/coating thickness, coverage values, and shape of the fine lines on prints.<sup>14</sup> However, this trend was not followed by both polar and dispersive components of  $\gamma$ . Specifically, the decrease of the polar component of  $\gamma$  after certain period proved as a tool for the fine adjustment of the coverage value and ink/coating thickness. Differential scanning calorimetry (DSC) and Thermogravimetric analysis (TGA), together with the swelling experiments, pointed to the breaking point between the crosslinking and the start of the changes in the types and quantity of bonds in the material caused by UV post-treatments. Fourier-transform infrared spectroscopy – Attenuated total reflectance (FTIR-ATR) analysis pointed to the changes in the photo polymeric material's surface composition: the decreased transmittance of oxygen-containing bonds. This change affected the polar component of  $\gamma$ . The weight loss obtained by means of the swelling experiments highly correlated with dispersive component of  $\gamma$ . Analysis of prints proved that the fine adjustments of UVA and UVC post-treatments result with significant changes in the high coverage values, deposited ink/coating thickness, and the shape of the fine printed elements.

## EXPERIMENTAL

### Sample Preparation

In this research, styrene-diene-styrene based photo polymeric material obtained by MacDermid was used as a flexographic

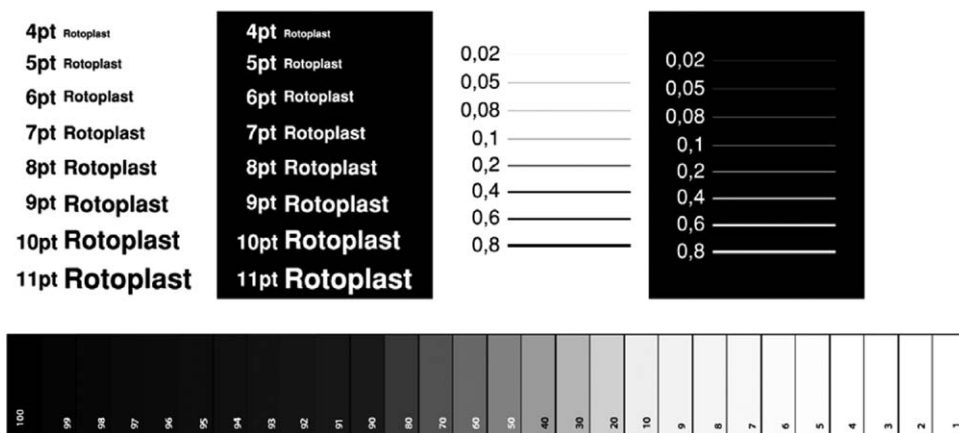


Figure 2. Digital test image transferred to the printing plate surface.

printing plate with height of 1.14 mm. The chemical and surface properties of the material were subject to change due to the variations in the post-treatment process. Photo polymeric material used as the printing plate was composed of styrene-diene-styrene copolymer with plasticizer (78%–92%), acrylic ester monomer (4%–14%), photoinitiator (1%–4%), and plasticizer butylated hydroxytoluene (BHT) (1%).<sup>23</sup> Printing plate samples were laser ablation mask layer (LAMS)-based, with digital Computer to Plate (CtP) production procedure.<sup>1</sup> Printing plate samples were produced using the standard procedure recommended by the manufacturer, up to the post-treatment process: the back-exposure was performed in Cyrel 1000 ECDLF unit for 70 sec at actinic wavelength of 365 nm and UV lamp intensity of 16 mW [Figure 1(b)], followed by the ablation of the mask layer in Esko Spark 4835 image setter [Figure 1(c)]. Main exposure [Figure 1(d)] was performed in Cyrel 1000 ECDLF unit for 10 min, at the same UV radiation properties as the back-exposure. Rinsing process was performed by means of Solvit QD solution, for 300 sec and at 20 °C, in the BASF COMBI FIII unit. The drying process was carried out in Cyrel 1000 ECDLF unit, at 60 °C and the duration of 120 min.<sup>24</sup> Test image transferred to the printing plate surface consisted of the control strip and the fine lines (Figure 2).

After the rinsing, stabilization period of printing plate in duration of 24 h was necessary to ensure the evaporation of the remaining solvent from the printing plate and to decrease the printing plate temperature to the operational temperature (20 °C). After the stabilization, produced printing plate samples were exposed to different durations of UVA and UVC post-treatments. Duration of the post-treatments varied from 0 to 20 min, with the step of 1 min.

The purpose of this research was to retain the necessary functional properties (printability) of the flexographic printing plate. To achieve that, both types of UV post-treatments had to be performed on the samples (except for the first sample, without any post-treatment which could not be used in the printing process, but only for the analysis of the chemical and surface properties; and second samples in set which were produced without one type of UV post-treatment). For the rest of the samples, duration of one type of post-treatment (UVA or UVC) was varied,

while other was kept fixed, at a standard value according to manufacturer's recommendations (Table I). Actinic wavelength of UVC lamps was 254 nm, and the lamp intensity was 9 mW.

Test prints produced by means of UV post-treated printing plate samples were obtained by printing machine Miraflex CM in standard conditions, in respect to the ISO 9001:2008 and ISO 14001:2004 standards.<sup>25,26</sup> Ethanol based printing ink from Gecko<sup>®</sup> Base was used in the printing process and 60  $\mu\text{m}$  low density polyethylene (PE LD) white was used as a printing substrate.<sup>27</sup>

It is important to notice that the interaction between the printing plate, the ink, and the substrate depends on the types of used materials. This research displays an experimental guideline for the application of UV post-treatments of flexographic photo polymeric materials to improve the print quality. Based on the other components of flexographic reproduction system, the duration of the UV post-treatments of flexographic printing plate surface can be adjusted to different durations than the ones applied in this research.

#### Materials, Methods and Devices

**Surface Free Energy Calculation.** To calculate the surface free energy ( $\gamma$ ) of photo polymeric surface, contact angles of chosen probe liquids on the flexographic printing plate needed to be determined. Contact angle and  $\gamma$  of the probe liquids are the parameters which are then used to calculate the  $\gamma$  of the solid samples.<sup>28</sup> Contact angle measurements were performed on DataPhysics OCA 30 Instruments GmbH device, at 20 °C.<sup>29</sup> Three probe liquids of known  $\gamma$  at 20 °C were used for the measurements: water (distilled twice;  $\kappa = 1.33 \mu\text{S/cm}$ ), glycerol (> 99.5% GC, Fluka), and diiodomethane (p.a. 99%, Aldrich).

Table I. Sets of Photo Polymeric Material Samples Treated with Varied UVA and UVC Radiation

|                          | SET 1                          |
|--------------------------|--------------------------------|
| UVA post-treatment (min) | 0, 0, 1, 2, ..., 18, 19, 20    |
| UVC post-treatment (min) | 0, 10, 10, 10, ..., 10, 10, 10 |
|                          | SET 2                          |
| UVA post-treatment (min) | 0, 10, 10, 10, ..., 10, 10, 10 |
| UVC post-treatment (min) | 0, 0, 1, 2, ..., 18, 19, 20    |

Contact angle was measured using Sessile drop method, 10 times on each sample, on the different parts of the printing plate. The shape of the probe liquid drops was a spherical cap and the volume of the drops was 1  $\mu\text{L}$ . All measurements of the contact angle on the samples were performed in the same moment after the drop touched the photopolymer surface – with delay of 10 frames and average value was calculated.

After obtaining the values of contact angles for each probe liquid, mean values of contact angle for each sample were calculated. The surface free energy ( $\gamma$ ) was calculated using Owens, Wendt, Rabel and Kaelble (OWRK) method, applicable for polymer, aluminum, and coatings characterization.<sup>28,29</sup>

**Differential Scanning Calorimetry (DSC).** DSC was used to display changes of photo polymeric material's heat capacity in dependence on the temperature.<sup>30</sup> DSC measurements were performed using Mettler Toledo DSC 823e unit. About 10 mg of sample was placed in the DSC unit and analyzed to characterize transitions in photo polymeric material and detect potential changes in those transitions caused by variations of UV post-treatments (crosslinking, degradation). All measurements were performed in nitrogen atmosphere ( $50 \text{ cm}^3 \text{ min}^{-1}$ ), and heating rate of  $10 \text{ }^\circ\text{C min}^{-1}$ . The specimens were heated from  $25 \text{ }^\circ\text{C}$  to  $350 \text{ }^\circ\text{C}$ . Heat effects as a function of temperature were detected in the interval between  $140 \text{ }^\circ\text{C}$  and  $340 \text{ }^\circ\text{C}$ .

**Thermogravimetric Analysis (TGA).** TGA is a technique used for thermal characterization of various materials. In this research, the rate and dynamics of weight loss of the photo polymeric material was displayed by thermal curves to analyze the potential amount of the residue after the heating and thermal stability and degradation of the photopolymer exposed to various durations of UV post-treatments.<sup>31</sup> TGA was carried out on a TA instrument Q500 at a temperature range from  $25 \text{ }^\circ\text{C}$  to  $900 \text{ }^\circ\text{C}$  at a heating rate of  $10 \text{ }^\circ\text{C min}^{-1}$  under the nitrogen atmosphere ( $50 \text{ cm}^3 \text{ min}^{-1}$ ). Targeted mass of the specimens was 10 mg.

**FTIR-ATR Spectroscopy.** FTIR-ATR spectroscopy is a technique used to identify the presence of certain functional groups in the molecule. Vibrations and rotations at a certain wavelength in the IR area are detected by IR spectrometry and can help in determining molecular composition and impurities in the sample.<sup>32</sup> In this research, FTIR-ATR was used to primarily identify the changes in the representation of the oxygen-containing and carbon–hydrogen bonds in the photo polymeric material exposed to UV post-treatments. The interpretation of FTIR-ATR spectra was used to back up, explain, and integrate the results obtained by other measurement and analysis techniques used in this work. Fourier transform infrared spectra were recorded using Perkin Elmer Spectrum One spectrometer. The spectra in the attenuated total reflectance mode (FTIR-ATR) for all samples were recorded in  $600\text{--}4000 \text{ cm}^{-1}$  frequency region using a Single Reflection ATR System ZnSe lens. The spectra were collected with a resolution of  $4 \text{ cm}^{-1}$  by co-adding the results of four scans. Background spectrum was collected before each measurement.

**Swelling Experiments.** Swelling measurements were performed by gravimetric method, in a controlled environment with a constant temperature of  $20 \text{ }^\circ\text{C}$ .<sup>33</sup> Acetone [capillary gas chromatography (GC) grade], ethyl acetate [American Chemical Society (ACS) grade], and toluene [American Chemical Society (ACS) reagent] were used as swelling agents due to the different types and strengths of their molecular bonds, and therefore different impact on the photo polymeric material. Named swelling agents cause swelling and partial dissolution of the photo polymeric material used in the printing plate production. Furthermore, ethyl acetate is a common solvent in flexography, specifically in the composition of printing inks and as a solution for cleaning the ink from the photopolymer plate.<sup>34</sup> Its usage needs to be therefore regulated, and the impact of the ethyl acetate on the treated photo polymeric material was therefore the most relevant point of this experiment, with acetone and toluene used to gain detailed insight in the photopolymer swelling behavior.

Photopolymer samples were immersed in the acetone, ethyl acetate, and toluene for periods up to 420 min, after which the weighing showed that the equilibrium of swelling was reached. Normalized degree of swelling ( $M_t$ ) for control periods of 5, 15, 30, 60, 90, 120, 180, 360, and 420 min of immersion were calculated using eq. (1):

$$M_t = \frac{m_t - m_0}{m_0} \times 100\% \quad (1)$$

where  $m_t$  stands for the weight of the swollen polymer at a time  $t$  and  $m_0$  for the mass of the dry polymer sample before the immersion. Before the initial immersion and after immersions, samples were dried at  $80 \text{ }^\circ\text{C}$  by means of OHAUS MB 45 moisture analyzer, after which the solvent ratio in the sample decreased to  $0.23\% \pm 0.01\%$  and stabilized. Samples were then weighted again to determinate the weight loss after the swelling.

**Analysis of Prints.** Coverage values (the optically effective portions of control area covered with printed elements) and ink/coating thickness on prints were measured 20 times on different spots on the prints to ensure correct calculations of the error.<sup>35</sup> For the observation of fine printed lines quality (width of  $20 \mu\text{m}$ ) in dependence on UV treatments, Olympus BX51 metallurgical microscope was used. For the measurement of coverage values on prints, IC Plate II was used. It is a portable device for visual analysis of different types of printing plates and prints. Its precise measurement of coverage values on test prints examined in this research enabled obtaining precise results in the coverage area higher than 90%. Ink/coating thickness on samples was measured by means of SaluTron D4-Fe. The gauge SaluTron D4-Fe works on the magnetic induction principle and measures all nonmagnetic coatings such as synthetics, lacquers, enamels, copper, chromium, zinc, etc. on steel or iron. Results of the measurements were used to identify the influence of variations of printing plate's  $\gamma$  on the quality of prints.

## RESULTS AND DISCUSSION

### Surface Free Energy Calculation

The surface free energy ( $\gamma$ ) calculations showed that the variations in UVA and UVC post-treatments have a similar effect on the photo polymeric material samples (Figures 3 and 4).

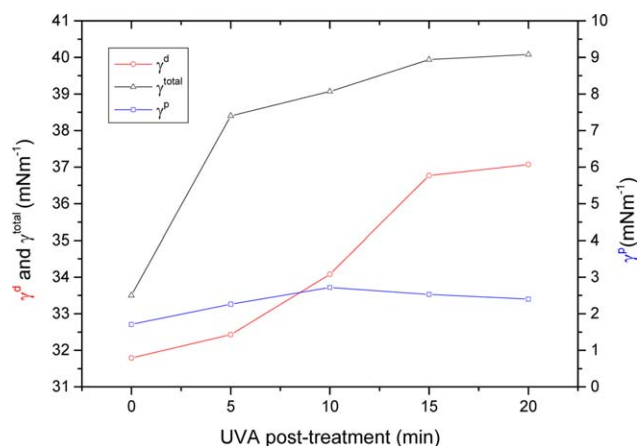


**Figure 3.** Effect of the UVA radiation on  $\gamma^{total}$ ,  $\gamma^p$ , and  $\gamma^d$  of the photo polymeric printing plate. [Color figure can be viewed in the online issue, which is available at wileyonlinelibrary.com.]

However, changes in  $\gamma$  caused by prolonged UVC post-treatment are more expressed than the changes caused by UVA radiation, since UVC radiation carries more energy.

The causes of the changes in  $\gamma$  and its components, together with the detection of the possible material degradation caused by UV post-treatments (and could affect its functional properties in the long run) are explained and defined by the analysis and measurement methods described in this paper.

Variation of the duration of the UVA post-treatment of the photo polymeric material from 0 to 20 min causes the increase of  $\gamma^{total}$  from  $33.5 \text{ m Nm}^{-1}$  to  $41.2 \text{ m Nm}^{-1}$  (Figure 3). Specifically, the increase of  $\gamma^d$  (from  $31.79 \text{ m Nm}^{-1}$  to  $37.07 \text{ m Nm}^{-1}$ ) with prolonged UVA radiation primarily causes the increase of  $\gamma^{total}$ . This behavior of the photo polymeric material can be explained by further crosslinking, which occurs in the photo polymeric material, and indicates that, even after the printing plate is considered to be finished in its production process, further crosslinking caused by UVA radiation takes place. However,  $\gamma^p$  increases only slightly, from  $1.71 \text{ m Nm}^{-1}$  to  $2.4 \text{ m Nm}^{-1}$  during the performed variations of the UVA radia-

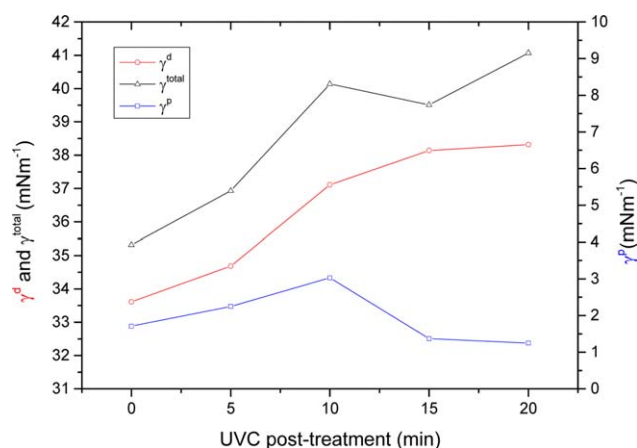


**Figure 4.** Effect of the UVC radiation on  $\gamma^{total}$ ,  $\gamma^p$ , and  $\gamma^d$  of the photo polymeric printing plate. [Color figure can be viewed in the online issue, which is available at wileyonlinelibrary.com.]

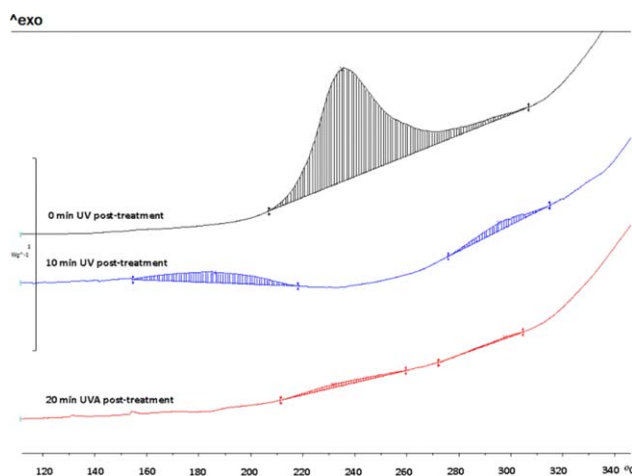


**Figure 5.** Display of exothermic reactions in photo polymeric material in dependence on UVA post-treatment duration obtained by DSC. [Color figure can be viewed in the online issue, which is available at wileyonlinelibrary.com.]

tion. Therefore, UVA radiation can be used as a tool to adjust  $\gamma^d$  of this specific photo polymeric material, but not as a tool to enhance significantly the adsorption of polar coatings.

On the other hand, prolonged UVC post-treatment (Figure 4) has a more expressed effect on all components of  $\gamma$ .

When varying the duration of the UVC radiation from 0 to 20 min,  $\gamma^{total}$  of the photo polymeric surface increases from  $33.5 \text{ m Nm}^{-1}$  to  $41.2 \text{ m Nm}^{-1}$ . Furthermore, even though  $\gamma^d$  (which increases from  $33.61 \text{ m Nm}^{-1}$  to  $38.32 \text{ m Nm}^{-1}$ ) is a dominant component influencing  $\gamma^{total}$ , changes in  $\gamma^p$  have an interesting trend.  $\gamma^p$  increases from  $1.71 \text{ m Nm}^{-1}$  at 0 min to  $3.03 \text{ m Nm}^{-1}$  at 10 min of the UVC radiation. After that,  $\gamma^p$  decreases to  $1.25 \text{ m Nm}^{-1}$  at 20 min of UVC radiation. This could be explained by the process of the migration of small carbohydrate compounds, such as unreacted monomers and protective waxes added to these types of photopolymers to the surface of the material.<sup>35,36</sup> Therefore, when the adjustment of  $\gamma^p$  of the flexographic printing plate surface is needed, initial test needs to be performed to detect the inflexion point with maximal  $\gamma^p$ .

However, since UVA radiation initiates the crosslinking reaction and UVC terminates it (due to the higher energy and generation of ozone), one should use both post-treatments and combine their duration to achieve desired  $\gamma$ . At the same, the functionality of the photo polymeric printing plate in the reproduction process must not be diminished.<sup>37,38</sup>

### Thermal Analysis of Photo Polymeric Material

**DSC Analysis.** Figures 5 and 6 display the temperature shift of the exothermic reactions in photo polymeric flexographic printing plate exposed to the varied durations of the UVA and UVC post-treatments. Photo polymeric material sample not treated with any UVA and UVC post-treatment shows one large peak at  $235.30 \text{ }^\circ\text{C}$ . This could point to the further heat-induced crosslinking reaction in the sample.<sup>39</sup> However, with prolonged UV post-treatments, separation to two exothermic peaks occurs, with the shift of the first peak to the lower temperatures. The energy released in the exothermic reaction decreases, which

**Table II.** Characteristics of DSC Curves for UV Post-Treated Photo Polymeric Material Samples

|               | 0 min UV | 10 min UV<br>(1st peak) | 10 min UV<br>(2nd peak) | 20 min UVA<br>(1st peak) | 20 min UVA<br>(2nd peak) | 20 min UVC<br>(1st peak) | 20 min UVC<br>(2nd peak) |
|---------------|----------|-------------------------|-------------------------|--------------------------|--------------------------|--------------------------|--------------------------|
| Integral (mJ) | 785.13   | 104.28                  | 39.65                   | 23.41                    | 5.11                     | 99.21                    | 10.28                    |
| Onset (°C)    | 218.62   | 154.65                  | 278.62                  | 211.47                   | 272.19                   | 186.82                   | 283.38                   |
| Peak (°C)     | 235.30   | 185.96                  | 295.67                  | 232.10                   | 297.97                   | 189.58                   | 294.65                   |
| Endset (°C)   | 262.78   | 211.36                  | 306.72                  | 260.16                   | 305.28                   | 213.38                   | 304.62                   |

corresponds to the increase of the crosslinking degree in the samples. Energy of reactions, peaks, onsets, and endsets are given in Table II.

Table II presents the temperatures of the peaks on DSC curves for analyzed photopolymer samples and corresponding energies for each exothermic peak. The energy of the first peak for the exothermic reaction for sample treated with 10 min of UVA and UVC post-treatment equals 13.28% of the energy corresponding to the non-treated sample. Furthermore, sample treated with 20 min of UVA post-treatment displays the energy of the first peak that equals 2.98% of the corresponding energy of the non-treated sample, and for the sample treated with 20 min of UVC post-treatment, it equals 12.64% of the corresponding energy of the non-treated sample. The gradual decrease of the released energy for 10 and 20 min of UVA post-treatment (Figure 5) indicates that the smaller amount of non-crosslinked compounds remain in the photo polymeric material after UV post-treatments, since UVA radiation induces crosslinking in the sample and triggers the reaction of crosslinkable parts. As the UVC post-treatment terminates the crosslinking reaction, there is no significant difference between first peaks for 10 and 20 min of UVA post-treatment (Figure 6).

Second peaks occurring on DSC displays of UV post-treated samples at cca. 295 °C point to the conclusion that UV post-treatments result with the formation of the two-phase system: the surface and the bulk of the photo polymeric material. The second exothermic peaks visible at 10 and 20 min for both UV post-treatments could therefore correspond to the reaction involving the hydroxyl group, which is the only new bond appearing in the photo polymeric material composition of the UV-treated samples and is visible in FTIR-ATR spectra in Figures 8 and 9.<sup>40</sup>

**TGA Measurements.** Figure 7(a–d) present the thermogravimetric (TG) and derivative thermogravimetric (DTG) curves for the tested photo polymeric material. They were displayed to show that UV post-treatments up to 20 min do not cause significant changes in the thermal stability of the material. The degradation rate is similar for all displayed samples, pointing to two steps of the weight loss (TG curve) starting at approx. 110 °C and 395 °C.

The derivative weight change (DTG curves) display the maximal temperature decomposition between approx. 430 °C and 450 °C with two close peaks, while the first peak at approx. 130 °C – 160 °C precedes the exothermic reaction displayed in DSC analysis results. This peak could be the consequence of the evaporation of low molecular weight compounds (the decomposition of

the tested photo polymeric material can take place above 200 °C).<sup>23</sup>

Furthermore, the residue after the heating is present only for the sample exposed to UV post-treatments for 10 min (2.4%). This shows that prolonged UV post-treatment affects the thermal decomposition of the photo polymeric material and causes the production of thermally non-degradable compounds, but only up to certain duration. After that, UV-induced reactions taking place in the material result with no residue after the thermal decomposition. This could be a valid note when considering the waste management.

#### FTIR-ATR Analysis

FTIR-ATR analysis of the photo polymeric material treated with varied durations of UV post-treatments primarily displayed the changes in the area of oxygen-containing bonds and secondly, in the area of CH<sub>2</sub> and C–H vibrations.

Specifically, in both Figures 8 and 9, with prolonged UV post-treatment, one can notice the changes in transmittance around 1750 cm<sup>-1</sup>, which corresponds to carbonyl bond vibration. Changes are visible in the wavenumber area of 3200 cm<sup>-1</sup> to 3500 cm<sup>-1</sup>, which corresponds to hydroxyl bond stretching.<sup>40</sup> The transmittance in these areas decreases with prolonged UV radiation and the change is more expressed with the increased duration of the UVC post-treatment (Figure 9).

However, both UVA and UVC post-treatments result with the increase in the transmittance of wavenumber areas at

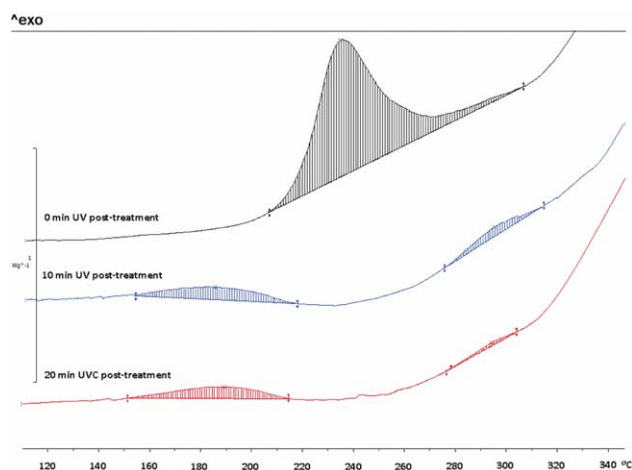


**Figure 6.** Display of exothermic reactions in photo polymeric material in dependence on UVC post-treatment duration obtained by DSC. [Color figure can be viewed in the online issue, which is available at [wileyonlinelibrary.com](http://wileyonlinelibrary.com).]

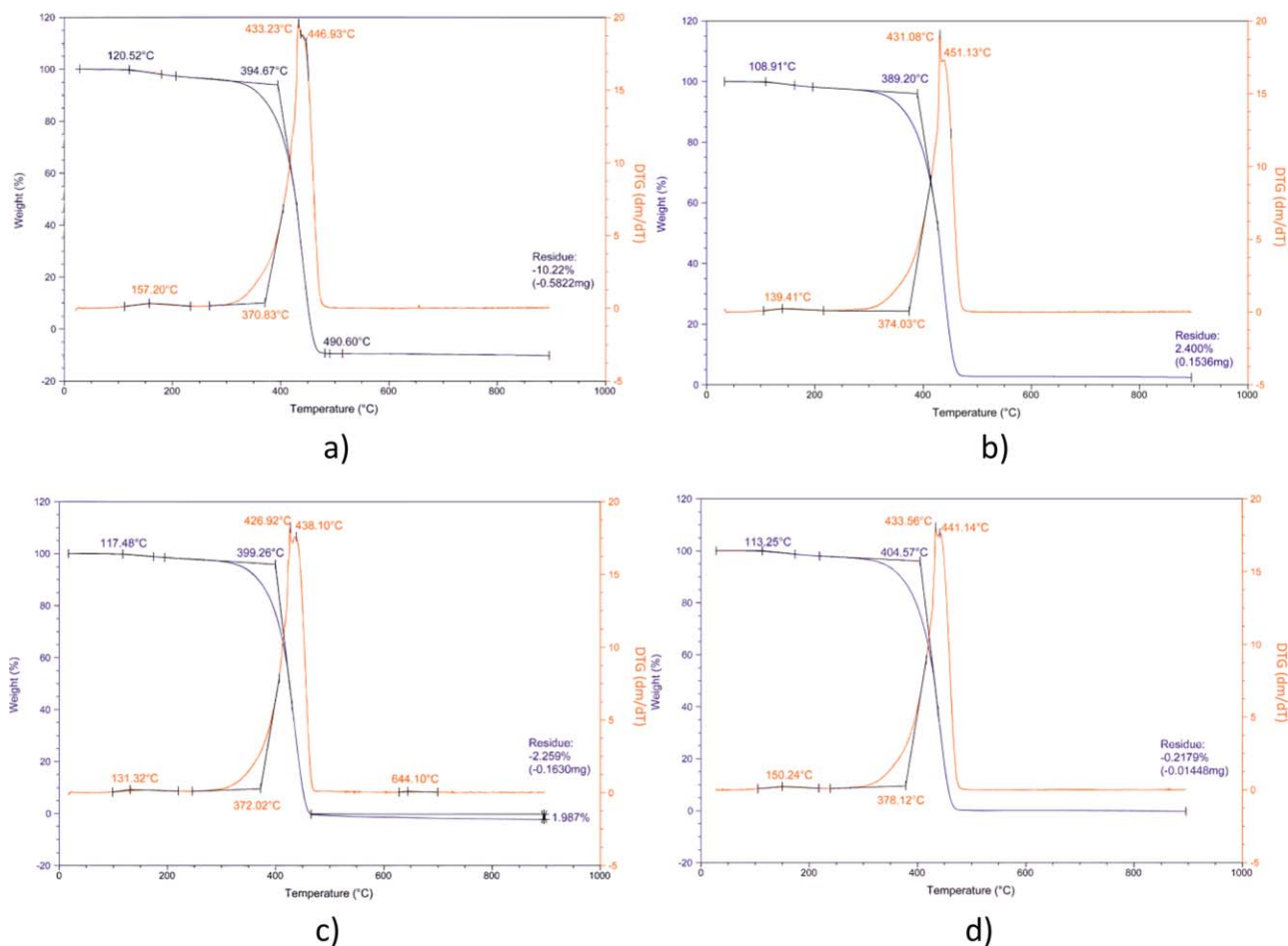


**Figure 7.** Display of TGA analysis on photo polymeric samples treated with: (a) 0 minutes of UV post-treatments, (b) 10 minutes of UV post-treatments, (c) 20 minutes of UVA post-treatment, and (d) 20 minutes of UVC post-treatment. [Color figure can be viewed in the online issue, which is available at [wileyonlinelibrary.com](http://wileyonlinelibrary.com).]

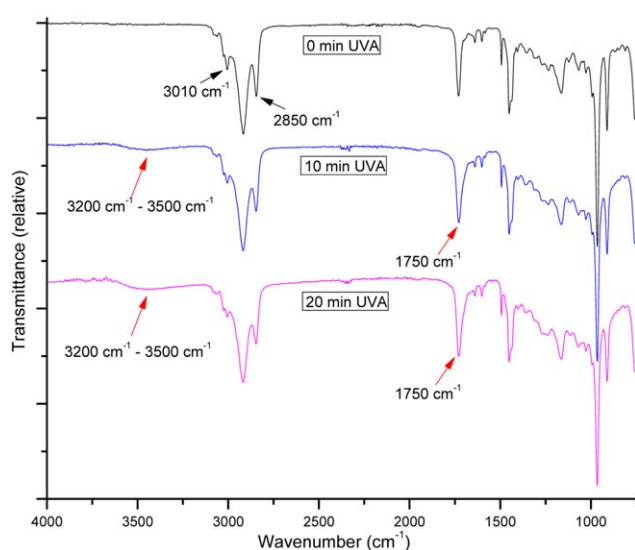


**Figure 8.** FTIR-ATR analysis of photo polymeric samples treated with varied duration of UVA post-treatment. [Color figure can be viewed in the online issue, which is available at [wileyonlinelibrary.com](http://wileyonlinelibrary.com).]

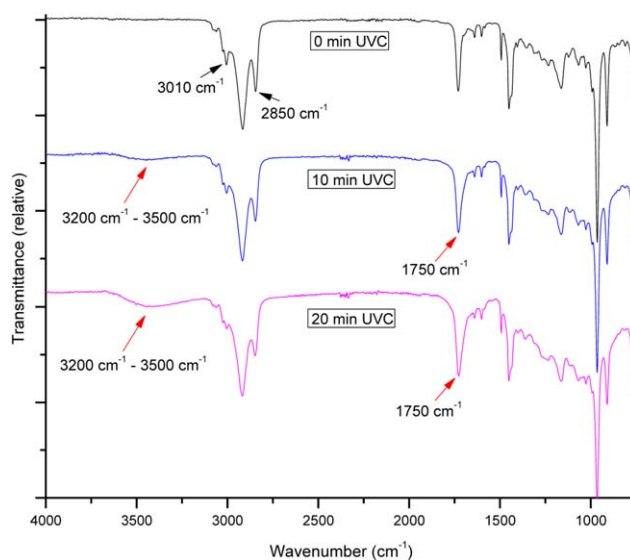


**Figure 9.** FTIR-ATR analysis of photo polymeric samples treated with varied duration of UVC post-treatment. [Color figure can be viewed in the online issue, which is available at [wileyonlinelibrary.com](http://wileyonlinelibrary.com).]

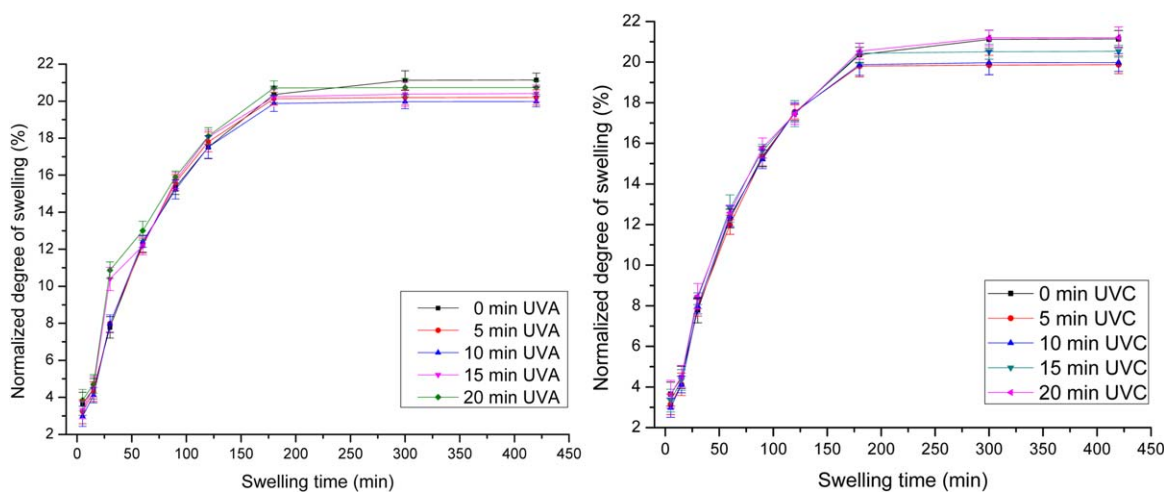


**Figure 10.** Normalized degrees of swelling for UV post-treated samples immersed in acetone for: (a) varied UVA post-treatment and (b) varied UVC post-treatment. [Color figure can be viewed in the online issue, which is available at [wileyonlinelibrary.com](http://wileyonlinelibrary.com).]

2850  $\text{cm}^{-1}$  and 3010  $\text{cm}^{-1}$ . These areas correspond to the C–H stretching.<sup>41</sup> The increase of transmittance at 3010  $\text{cm}^{-1}$  can be interpreted as a confirmation of the further crosslinking in the photo polymeric material caused by both UVA and UVC radiation, since the C–H stretch in this area can be interpreted as a sign of the unsaturation in the compound.<sup>41</sup> However, the increase of the transmittance at 2850  $\text{cm}^{-1}$ , which belongs to saturated systems, points to the changes in structure of the photo polymeric network, which could be a consequence of the crosslinking termination/photooxidation reactions.<sup>41</sup>

### Swelling Experiments

Figures 10–12 present the normalized degrees of photopolymer swelling in different solvents depending on the durations of UV post-treatments.

The general behavior of photopolymer swelling shows the similar trend for the immersion in all solvents, but with different normalized degree of swelling. Generally, the degree of swelling decreases with UVA and UVC post-treatments for durations up to 5–10 min and then increases, reaching the equilibrium at

approx. 420 min of immersion for all samples. Normalized degree of swelling in acetone (Figure 10) reaches maximal value of 20.72% at 20 min of UVA post-treatment and a similar value of 21.21% at 20 min of UVC post-treatment. On the other hand, swelling in ethyl acetate (Figure 11) is less expressed, with maximum of 1.08% for non-UV post-treated sample and 1.20% for sample treated with UVC radiation for 20 min.

General increase of the normalized degree of swelling after 10 min of UV post-treatments can be associated with the simultaneous decrease of the  $\gamma^p$  (which is specifically expressed after 10 min of UVC post-treatment [Figures 3 and 4] and the increase of  $\gamma^d$ , since the solvent first needs to penetrate the surface of the photo polymeric material.

However, the maximal normalized degree of swelling in toluene (Figure 12) is 8.32 times higher than in acetone and 147.12 times higher than in ethyl acetate. Toluene is a solvent with hydrogen bonding component of 2.0  $\text{MPa}^{1/2}$  according to Hansen parameters scale, while hydrogen bonding component amounts 7.0  $\text{MPa}^{1/2}$  for acetone and 7.2  $\text{MPa}^{1/2}$  for ethyl

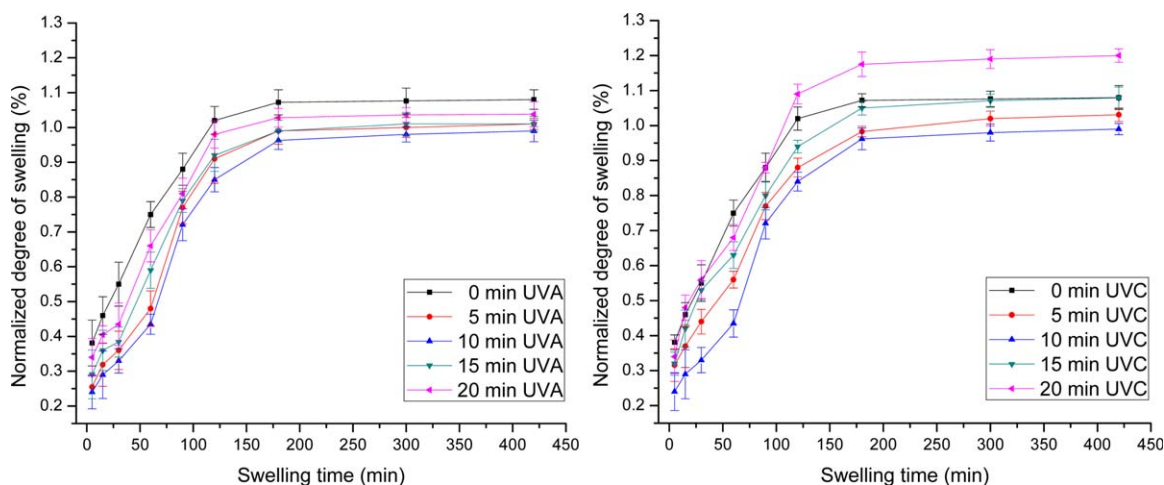


**Figure 11.** Normalized degrees of swelling for UV post-treated samples immersed in ethyl acetate for: (a) varied UVA post-treatment and (b) varied UVC post-treatment. [Color figure can be viewed in the online issue, which is available at [wileyonlinelibrary.com](http://wileyonlinelibrary.com).]



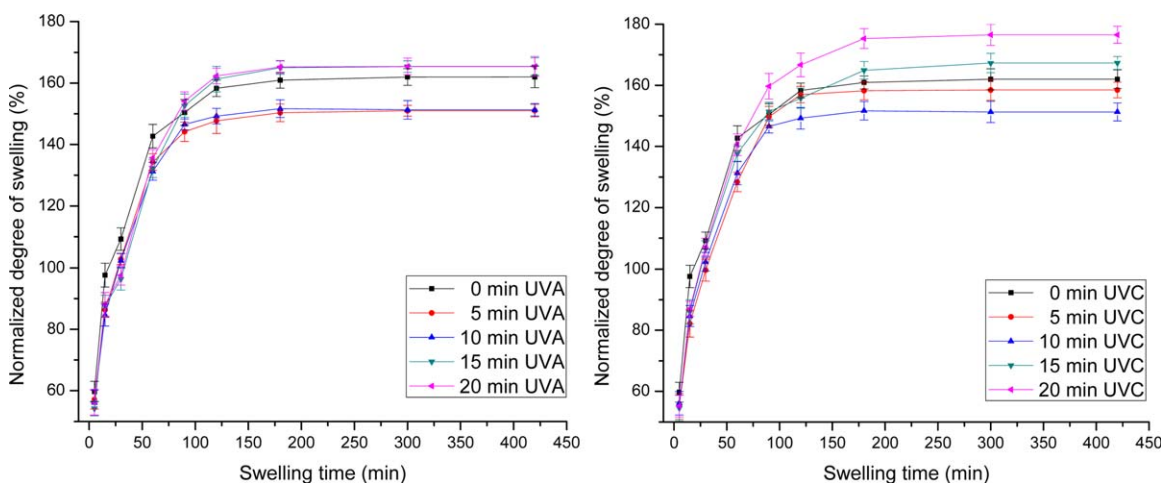


**Figure 12.** Normalized degrees of swelling for UV post-treated samples immersed in toluene for: (a) varied UVA post-treatment (b) varied UVC post-treatment. [Color figure can be viewed in the online issue, which is available at [wileyonlinelibrary.com](http://wileyonlinelibrary.com).]

acetate. Furthermore, the Hansen's polar component for toluene equals  $1.4 \text{ MPa}^{1/2}$ ,  $10.4 \text{ MPa}^{1/2}$  for acetone, and  $5.3 \text{ MPa}^{1/2}$  for ethyl acetate. Hansen's dispersion component for toluene equals  $18 \text{ MPa}^{1/2}$ ,  $15.5 \text{ MPa}^{1/2}$  for acetone, and  $15.8 \text{ MPa}^{1/2}$  for ethyl acetate. Total Hildebrand parameters for used solvents are:  $20.0 \text{ MPa}^{1/2}$  for acetone,  $18.1 \text{ MPa}^{1/2}$  for ethyl acetate, and  $18.2 \text{ MPa}^{1/2}$  for toluene.<sup>42</sup>

This indicates that swelling of the photo polymeric material in toluene shows the highest values due to the similar cohesion parameter of soluble component of photo polymeric material and the solubility parameters of toluene, in relation to the dispersion force and low value of polar force of toluene. Furthermore, it can be concluded that the photo polymeric material used in this research does not display the hydrogen bonding capability.

Changes in the photo polymeric material weight loss after the swelling in different solutions [Figure 13(a,b)] present the general decreasing trend and, together with the other results obtained in this research, point to the conclusion that the changes which occur on the surface of the photo polymeric

material as a consequence of the UV post-treatments differ from the changes in the bulk of the material.

Weight loss for samples exposed to varied UVA post-treatment and swelled in all three testing solvents decreases, as well as the weight loss of UVC post-treated samples. Specifically, samples swelled in toluene display the sharper decrease of the weight loss after 10 min of both UV post-treatments. This points to the expressed changes of the bond strengths in the photo polymeric material volume after that point. Therefore, it can be concluded that both UVA and UVC post-treatments cause further cross-linking in the volume of the photo polymeric material, resulting with material more resistant to dissolution. This decreases the possibility of damaging the flexographic printing plate during the exploitation process, when printing with solvent-based inks and washing the printing plate. However, although minimal, the swelling degree and weight loss in ethyl acetate should be monitored when using printing plate washing agents and inks containing ethyl acetate, as prolonged UV post-treatments cause the increased photopolymer swelling.

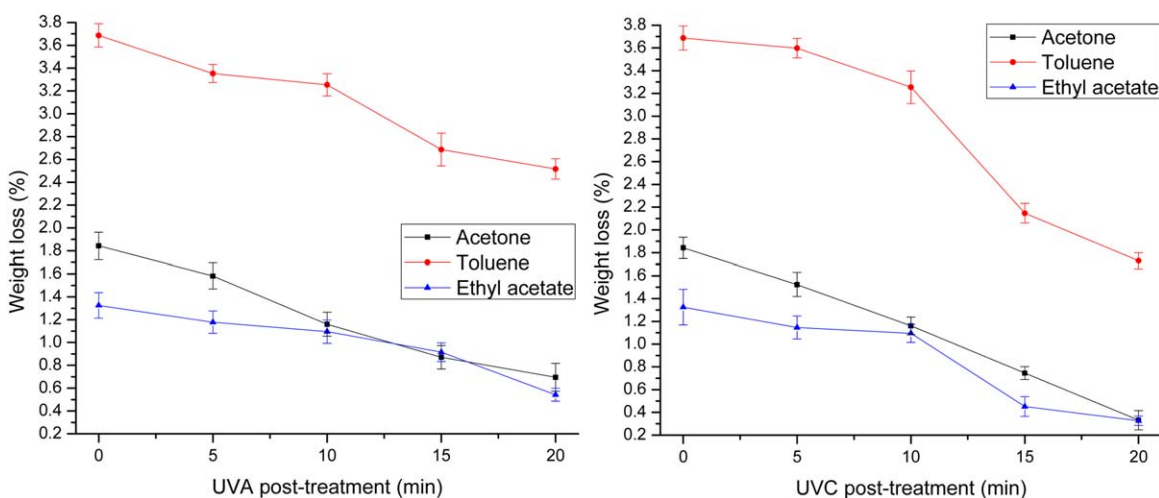


**Figure 13.** Weight loss of the photo polymeric material after swelling in dependence on the duration of: (a) UVA post-treatment and (b) UVC post-treatment. [Color figure can be viewed in the online issue, which is available at [wileyonlinelibrary.com](http://wileyonlinelibrary.com).]

**Table III.** Correlation Coefficients for Weight Loss (%) in Different Solvents and  $\gamma^d$  for UVA and UVC Post-Treated Photopolymer Samples

|                    | Acetone | Ethyl acetate | Toluene |
|--------------------|---------|---------------|---------|
| UVA post-treatment | -0.978  | -0.908        | -0.979  |
| UVC post-treatment | -0.950  | -0.883        | -0.889  |

Table III presents the Pearson correlation coefficients of  $\gamma^d$  for sets of UV post-treated samples and the corresponding weight loss in different solvents.

Pearson Product-Moment Correlation Coefficient ( $r$ ) was calculated according to eq. (2):

$$r = \frac{\sum_{i=1}^n ((x_i - \bar{x})(y_i - \bar{y}))}{\sqrt{\sum_{i=1}^n (x_i - \bar{x})^2 \sum_{i=1}^n (y_i - \bar{y})^2}} \quad (2)$$

Since  $\gamma^d$  of polymers can be influenced by the degree of crosslinking, the correlation coefficients were calculated to quantitatively connect the weight loss of the photo polymeric material used to assess the relations in crosslinking in the samples and  $\gamma^d$ , an important surface characteristic in the flexographic reproduction process.<sup>43</sup> Presented correlation is negative and strong for all solvents, which suggests that the crosslinking process in UV post-treated flexographic printing plate is a primary factor modifying  $\gamma^d$ , and can be simply used for the fine adjustment of  $\gamma^d$ .

#### Testing of UV Post-Treated Photo Polymeric Printing Plates and Application in Flexographic Deposition of Thin Coatings

To obtain the confirmation that UV modification increases the quality of thin coatings, the analysis of the prints obtained by UV post-treated photo polymeric printing plates has been performed.

**Quality of Fine Lines Printed by UV Post-Treated Printing Plates.** In Figure 14, one can see the effect of the varied UV post-treatments on the fine lines on prints. It is visible that the line printed by means of the printing plate without any UVA post-treatment results with poor transfer of the ink to the printing substrate. This indicates that  $\gamma$  of the photo polymeric material is too low at that point to be able to ensure the correct adsorption of the printing ink on the printing plate surface. Prolonged UVA post-treatment results with better definition of the line shape, since the UV post-treatment increases the hardness of the photo polymeric material, as well.<sup>44</sup> However, as the hardness of the printing plate increases and results with decreased elastic deformation of the printing plate during the engagement, together with the decrease of  $\gamma^p$  at 20 min of UVA post-treatment, the line on the print becomes thinner. Therefore, UVA post-treatment can be used to decrease the width of the printed fine elements (in coordination with specific printing ink and printing substrate used).

On the other hand, the absence of UVC post-treatment results with mechanical damage of the fine element on the printing plate during the engagement and the loss of the ink transfer to the printing substrate. Prolonged UVC post-treatment of the photo polymeric material will ensure stable, correctly defined line on the print. Since  $\gamma$  of the photo polymeric material increases with prolonged UVC treatment more than with prolonged UVA treatment,

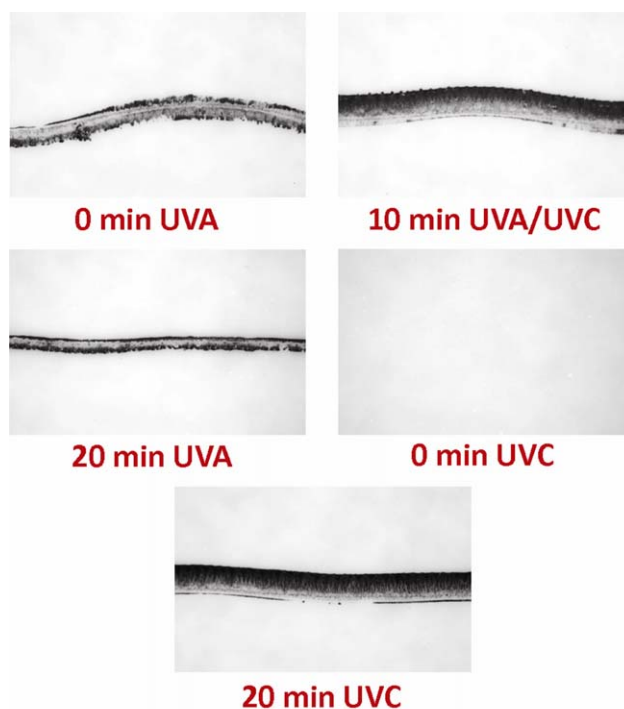


**Figure 14.** Lines with nominal width of 20  $\mu\text{m}$  (magnification of 50 $\times$ ) on prints obtained by printing plates exposed to varied UV post-treatments. [Color figure can be viewed in the online issue, which is available at wileyonlinelibrary.com.]

wetting of the printing plate with printing ink becomes improved, as well. Therefore, the width of the line will not be decreased and ink uniformity on the printed element will improve.

**Coverage Values on Prints Obtained by UV Post-Treated Printing Plates in 90%–100% Coverage Area.** Results displayed in Figure 15 are in conformity with the results of the fine lines analysis. UVA post-treated samples in the area of high surface coverage show the decreasing trend on the prints with prolonged UVA post-treatment [Figure 15(a)]. This means that the dot gain on the print decreases at longer UVA post-treatments. This is important for the reproduction of shadow areas on prints, as they can often end up as 100% coverage on the print, resulting with the loss of dark tonal values.<sup>45</sup>

On the other hand, UVC post-treatment results with the increased high coverage values on prints with printing ink used

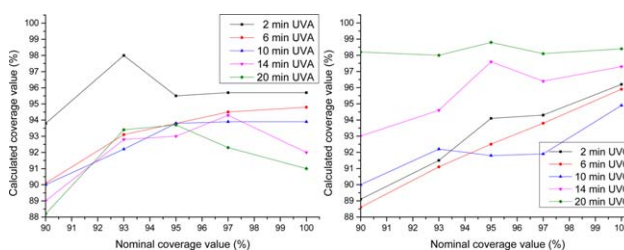


**Figure 15.** Values in high coverage area on prints obtained by: (a) set of varied durations in UVA post-treatment of printing plates and (b) set of varied durations in UVC post-treatment of printing plates. [Color figure can be viewed in the online issue, which is available at wileyonlinelibrary.com.]

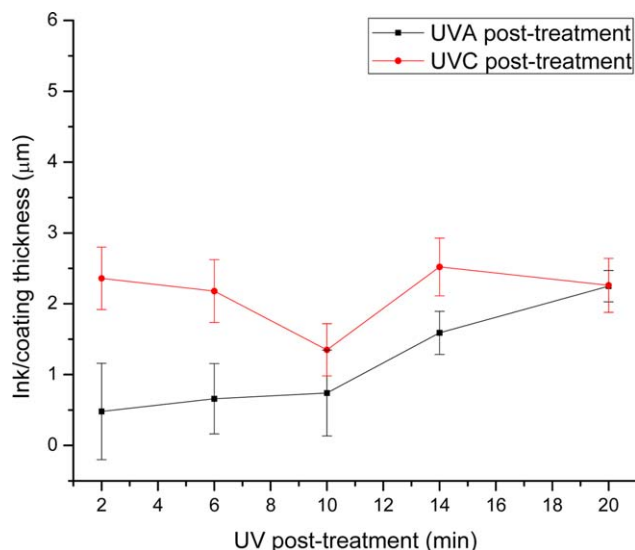


**Figure 16.** Ink/coating thickness on prints in dependence on UVA and UVC post-treatments. [Color figure can be viewed in the online issue, which is available at [wileyonlinelibrary.com](http://wileyonlinelibrary.com).]

in this research [Figure 15(b)] after 10 min. Therefore, if a solid tonal patch, with 100% coverage value needs to be printed, prolonged UVC post-treatment will result with best results. However, if the transitions in the shadow area are important for the specific print, the duration of the UVC post-treatment needs to be strictly regulated.

**Ink/Coating Thickness on Prints Obtained by UV Post-Treated Printing Plates.** Figure 16 presents the effect of the UVA and UVC post-treatments on the thickness of the ink/coating on the print – as discussed previously, a feature of crucial importance in many aspects of the functional printing. Lower duration of the UVA post-treatment results with the distinguished lower  $\gamma^d$  of the photo polymeric material, therefore resulting with poor wetting of the ethanol-based type of printing ink used in this research and transfer of the lower amount of the printing ink to the printing substrate.

The increased  $\gamma^{\text{total}}$  with prolonged UVA post-treatment is caused primarily by the increase of  $\gamma^d$  and will result with the thicker coating of printing ink on the printing substrate. However, according to the trend of the changes in the ink/coating thickness on prints obtained by printing plates treated with varied UVC post-treatments, one can conclude that  $\gamma^p$  has the main influence on lowering the ink/coating thickness. Pearson correlation coefficient for  $\gamma^p$  and deposited ink/coating thickness with varied UVC post-treatments is  $-0.89$ , which is a strong negative correlation and indicates that higher  $\gamma^p$  causes significant decrease of the deposited ink/coating thickness in this case.

This proves that, although the changes of the surface properties of flexographic printing plates due to the UV post-treatments may not appear as significant at a first glance, they greatly affect the quality of the deposition of the ink/coating on the printing substrate. Flexographic printing is a sensitive process, and minor changes of the photopolymer printing plate properties can reflect significantly on the final product. After testing and defining the

dynamics of the changes of deposited ink/coating parameters in dependence on the UV post-treatments, one can precisely adjust the qualitative and quantitative properties related to the print and obtain a tailored system applicable for the specific requirement.

## CONCLUSIONS

In this research, surface free energy of photo polymeric material used as flexographic printing plate was modified by means of UVA and UVC post-treatments to analyze and apply printing plate's changed properties for tailoring the features of the deposited printing ink/coating. Surface free energy calculations presented the general increase due to the prolonged UV post-treatments. However, polar component of surface free energy displayed the decrease after 10 min of both UVA and UVC post-treatments, expressed with prolonged UVC post-treatment. Although FTIR-ATR analysis showed the gradual increase of the oxygen-containing bonds portion, this behavior can be the effect of the migration of the smaller hydrocarbon compounds to the surface of the photo polymeric material. TGA analysis of the photo polymeric material has not displayed any negative changes in thermal stability of the material, while DSC analysis pointed to the decreased exothermic reactivity of the photo polymeric material with prolonged UV post-treatments due to the increased crosslinking degree. Swelling experiments displayed the closest relation between the cohesion parameter of photo polymeric material and cohesive energy density of toluene, but also pointed to the changes in the bond strengths in the material after 10 min of both UVA and UVC post-treatments. Weight losses after the swelling in solvents showed the decrease, which points to the further crosslinking reactions in the bulk of the photo polymeric material with longer UV post-treatments. Results of the weight loss measurements pointed to the conclusion that the flexographic printing plate and its properties should be analyzed as two different systems when exposed to the UV post-treatments: the surface and the bulk. Prints obtained by UV post-treated photo polymeric printing plates displayed significant changes in terms of the shape of the fine lines, coverage value, and the deposited ink/coating thickness. This research proved that the polar and dispersive component of the surface free energy affected by small changes in the durations of UVA and UVC post-treatments can be used as a quick and practical tool to define and precisely adjust the properties of the deposited ink/coating on the printing substrate. By applying described treatments of the flexographic printing plate, tailored flexographic reproduction system can be achieved without diminishing the printing plate's functionality and performing complicated (and often expensive) modifications of other components in the graphic reproduction process.

## REFERENCES

- Kipphan, H. *Handbook of Print Media*; Springer: Berlin, 2001; p 397.
- Choi, J.; Dasa, S.; Theodoreb, N. D.; Kimc, I.; Honsbergd, C.; Choie, H. W.; Alforda, T. L. *ECS J. Solid State Sci. Technol.* 2015, 4, 3001.

3. Lloyd, J. S.; Fung, C. M.; Deganello, D.; Wang, R. J.; Maffei, T. G. G.; Lau, S. P.; Teng, K. S. *Nanotechnology* **2013**, *24*, 195602. DOI: 10.1088/0957-4484/24/19/195602
4. Maksud, M. I.; Yusof, M. S.; Embong, Z.; Nodin, M. N.; Rejab, N. A. *Int. J. Mater. Sci. Eng.* **2014**, *2*, 49.
5. Ummartyotin, S.; Juntaro, J.; Wu, C.; Sain, M.; Manuspiya, H. *J. Nanomater.* **2011**, *2011*, 1.
6. Wang, Z. Ph.D. Thesis, University of California, Berkeley, spring **2013**.
7. Rentzhog, M.; Fogden, A. *Nord. Pulp Pap. Res. J.* **2006**, *21*, 202.
8. Pennaz, T. J.; Schuster, M. U.S. Pat. 20,120,171,547 A1, December 7 (**2010**).
9. Deng Xian, Y. *Int. J. Mol. Sci.* **2011**, *12*, 1575.
10. Buckley, A., Ed. *Organic Light-Emitting Diodes (OLEDs): Materials, Devices, and Applications*; Elsevier: London, **2013**; p 381.
11. Deganello, D.; Cherry, J. A.; Gethin, D. T.; Claypole, T. C. *Thin Solid Films* **2010**, *518*, 6113.
12. Klauk, H., Ed. *Organic Electronics: Materials, Manufacturing, and Applications*; Wiley: Weinheim, **2006**; p 259.
13. Johnson, J. Ph.D. Thesis, Karlstad University, **2008**.
14. Tomašegović, T.; Mahović Poljaček, S.; Cigula, T. *J. Print Media Technol. Res.* **2013**, *4*, 227.
15. Rentzhog, M. Ph.D. Thesis, Royal Institute of Technology, Stockholm, **2006**.
16. Durand, R. R., Jr.; Sprycha, R.; Mathew, M. Eur. Pat. 2,542,634 A1, March 1 (**2010**).
17. Duoss, E. B.; Twardowski, M.; Lewis, J. A. *Adv. Mater.* **2007**, DOI: 10.1002/adma.200701372.
18. Bollströma, R.; Tobjörka, D.; Dolietisa, P.; Salminen, P.; Prestona, J.; Österbackaa, R.; Toivakkaa, M. *Chem. Eng. Process. Process Intensif.* **2013**, *68*, 13.
19. Rentzhog, M. Licentiate Thesis, Royal Institute of Technology, Stockholm, **2004**.
20. Conners, T. E.; Banerjee, S. *Surface Analysis of Paper*; CRC Press: New York, **1995**, p 104.
21. Pekarovicova, A.; Husovska, V. In *Printing on Polymers: Fundamentals and Applications*; Izdebska, J., Thomas, S., Eds.; William Andrew: Waltham, **2015**, Chapter 3, p 49.
22. Feldman, D. *J. Polym. Environ.* **2002**, *10*, 163.
23. MacDermid Digital MAX – Photopolymer Plate Safety Data Sheet 91/155/EEC - 2001/58/EC - ISO 11014-1.
24. MacDermid Digital MAX Photopolymer Plates. Available at: [http://printing.macdermid.com/files/8514/2626/3635/Digital\\_MAX\\_092112.pdf](http://printing.macdermid.com/files/8514/2626/3635/Digital_MAX_092112.pdf) (accessed November 2, **2015**).
25. Implementation Guidance for ISO 9001:2008. Available at: [http://www.iso.org/iso/06\\_implementation\\_guidance.pdf](http://www.iso.org/iso/06_implementation_guidance.pdf) (accessed November 2, **2015**).
26. ISO 14001:2004 Environmental management systems – Requirements with guidance for use. Available at: [www.iso.org/iso/catalogue\\_detail?csnumber=31807](http://www.iso.org/iso/catalogue_detail?csnumber=31807) (accessed November 2, **2015**).
27. Gecko® Base Technical Information. Available at: <http://www.hubergroup.info/lang/en/tipdf/11P023en.pdf> (accessed November 2, **2015**).
28. Owens, D. K.; Wendt, R. C. *J. Appl. Polym. Sci.* **1969**, *13*, 1741.
29. Dataphysics – Product for Surface Chemistry. Available at: [http://www.laborexport.hu/pdf/DPI\\_Products\\_Overview\\_E.pdf](http://www.laborexport.hu/pdf/DPI_Products_Overview_E.pdf) (accessed November 2, **2015**).
30. Gregorova, A. Application of Differential Scanning Calorimetry to the Characterization of Biopolymers. <http://cdn.intechopen.com/pdfs-wm/42247.pdf> (accessed November 2, **2015**).
31. Characterization of Polymers Using TGA. Available at: [http://www.perkinelmer.com/CMSResources/Images/44-132088\\_APP\\_CharacterizationofPolymersUsingTGA.pdf](http://www.perkinelmer.com/CMSResources/Images/44-132088_APP_CharacterizationofPolymersUsingTGA.pdf) (accessed November 2, **2015**).
32. FT-IR Spectroscopy Attenuated Total Reflectance (ATR). Available at: [http://www.utsc.utoronto.ca/~traceslab/ATR\\_FTIR.pdf](http://www.utsc.utoronto.ca/~traceslab/ATR_FTIR.pdf) (accessed November 2, **2015**).
33. Liu, J.; Zheng, X. J.; Tang, K. Y. *Rev. Adv. Mater. Sci.* **2013**, *33*, 452.
34. Kaoru, F.; Hiroshi, H.; Fumio, I.; Yoshinobu, M.; Sakae, S.; Minoru, Y. Flexo Ink Composition, U.S. Pat. 3,912,675 A, October 14 (**1975**).
35. Knöll, R. Eur. Pat. 1158364 A2, May 3, **2000**.
36. Sakaguchi, Y.; Kawahara, K.; Yamada, T.; Okazaki, Y.; Imahashi, S. *J. Appl. Polym. Sci.* **2004**, *92*, 2903.
37. Kramer, P.; Davis, L.; Jones, R. Control of Free Radical Reactivity in Photopolymerization of Acrylates. Available at: [http://www.radtechmembers.org/2012-Papers/2012/papers/Session%2024%20-%20Kinetics/PKramer\\_Rutgers.pdf](http://www.radtechmembers.org/2012-Papers/2012/papers/Session%2024%20-%20Kinetics/PKramer_Rutgers.pdf) (accessed November 2, **2015**).
38. Yagci, Y.; Jockusch, S.; Turro, N. J. *Macromolecules* **2010**, *43*, 6245.
39. Sepe, M. P. *Thermal Analysis of Polymers*; iSmithers Rapra Publishing: Shawbury, **1997**; Vol. 8, Chapter 2, p 10.
40. Ishida, H.; Agag, T., Eds.; *Handbook of Benzoxazine Resins*; Elsevier: Amsterdam, **2011**; p 169.
41. Coates, J. In *Encyclopedia of Analytical Chemistry*; Meyers, R. A. Ed.; Wiley: Chichester, **2000**; p 10815.
42. Hansen, C. M. *Hansen Solubility Parameters: A User's Handbook*, 2nd ed; CRC Press: Boca Raton, **2007**; p 323.
43. Asmussen, E.; Attal, J. P.; Degrange, M. *J. Dent. Res.* **1995**, *74*, 715.
44. Mahović Poljaček, S.; Tomašegović, T.; Gojo, M. In *GRID 2012 Proceedings*, Novi Sad, Serbia, November 15–16, 2012; Novaković, D., Ed.; Faculty of Technical Sciences: Novi Sad, **2012**.
45. Tomašegović, T.; Mahović Poljaček, S.; Milčić, D. In *Proceedings of the 19th IAPRI World Conference on Packaging*, Melbourne, Australia, June 15–18, 2014; Sek, M. A., Rouillard, V.; Bigger, S. W., Eds.; Victoria University: Melbourne, **2014**.